White Rose Research Online

eprints@whiterose.ac.uk
https://eprints.whiterose.ac.uk
Universities of Leeds, Sheffield and York

Deposited via The University of Sheffield.

White Rose Research Online URL for this paper:
https://eprints.whiterose.ac.uk/id/eprint/134834/

Version: Accepted Version

Article:
Zhou, D., Pang, L.X., Wang, D.W. et al. (2018) High Quality Factor, Ultralow Sintering Temperature Li6B4O9 Microwave Dielectric Ceramics with Ultralow Density for Antenna Substrates. ACS Sustainable Chemistry and Engineering, 6 (8). pp. 11138-11143.

https://doi.org/10.1021/acssuschemeng.8b02755

Reuse
Items deposited in White Rose Research Online are protected by copyright, with all rights reserved unless indicated otherwise. They may be downloaded and/or printed for private study, or other acts as permitted by national copyright laws. The publisher or other rights holders may allow further reproduction and re-use of the full text version. This is indicated by the licence information on the White Rose Research Online record for the item.

Takedown
If you consider content in White Rose Research Online to be in breach of UK law, please notify us by emailing eprints@whiterose.ac.uk including the URL of the record and the reason for the withdrawal request.

UNIVERSITY OF LEEDS
University of Sheffield
UNIVERSITY of York

High quality factor, ultra-low sintering temperature $Li_6B_4O_9$ microwave dielectric ceramics with ultra-low density for antenna substrates

Di Zhou*[a,b], Li-Xia Pang[a,c], Da-Wei Wang[a], Ze-Ming Qi[d], & Ian M. Reaney*[a]

[a]Department of Materials Science and Engineering, University of Sheffield, Sir Robert Hadfield Building, Mappin Street, S1 3JD, UK

*Corresponding author email: zhoudi1220@gmail.com (Di Zhou)

*Corresponding author email: i.m.reaney@sheffield.ac.uk (Ian M. Reaney)

[b]Electronic Materials Research Laboratory, Key Laboratory of the Ministry of Education & International Center for Dielectric Research, School of Electronic and Information Engineering, Xi'an Jiaotong University, No. 28 Xian Ning West Road, Xi'an 710049, China

[c]Micro-optoelectronic Systems Laboratories, Xi'an Technological University, No. 6 Jinhua North Road,Xi'an 710032, Shaanxi, China

[d]National Synchrotron Radiation Laboratory, University of Science and Technology of China, Hezuo Hua South Road, Anhui, 230029, Hefei, China

Abstract

Dense $Li_6B_4O_9$ microwave dielectric ceramics were synthesized at low temperature via solid state reaction using Li_2CO_3 and $LiBO_2$. Optimum permittivity (ε_r) ~ 5.95, quality factor (Qf) ~ 41,800 GHz and temperature coefficient of resonant frequency (TCF) ~ −72 ppm/°C were obtained in ceramics sintered at 640 °C with a ultra-small bulk density ~ 2.003 g/cm^3 (~ 95% relative density, the smallest among all the reported microwave dielectric ceramics). $Li_6B_4O_9$ ceramics were shown to be chemically compatible with silver electrodes but reacted with aluminum forming $Li_3AlB_2O_6$ and Li_2AlBO_4 secondary phases. A prototype patch antenna was fabricated by tape casting and screen printing. The antenna resonated at 4.255 GHz with a bandwidth ~ 279 MHz at −10 dB transmission loss (S_{11}) in agreement with simulated results. The $Li_6B_4O_9$ microwave dielectric ceramic possesses similar microwave dielectric properties to the commercial materials but much lower density and could be good candidate for both antenna substrate and low temperature co-fired ceramics (LTCC) technology.

KEYWORDS: *Microwave Dielectric Ceramic, Low Temperature Co-Fired Ceramic Technology (LTCC), Patch Antenna, $Li_6B_4O_9$, Dielectric Substrate*

Introduction

Since the 'Internet of Things' (IoT) was first recognized by Ashton in 1999, it has driven a rapid increase in wirelessly connected devices, in areas as diverse as the home, transport, healthcare, military and oil / gas.[1-5] Mobile broadband, driven by the so called 3G/4G into 5G networks has seen in increase in data transmission rates, necessitating improvements in materials in critical components, such as antennas, filters and resonators.[1-6] For a ceramic material to be a dielectric passive substrate for antennas, resonators or filter, three properties need to be optimized: permittivity (ε_r); the temperature coefficient of the resonant frequency (*TCF*) and dielectric loss or rather its inverse, the quality factor Q, which is often multiplied by the resonant frequency, to give the material constant *Qf*. The electromagnetic wave length is inversely proportional to the square root of ε_r which means dielectric materials with high ε_r minimize device dimensions.[6-12] In 2007, Zhou et al.[13] designed a two-element antenna using $BiNbO_4$ ceramics (ε_r=43) as the substrate with an operating frequency about 3.5 GHz and dimensions 34 × 34 × 1 mm. However, due to the so called 'Chu-limit' the bandwidth was restricted to only 34 MHz at −10 dB, along with poor gain and efficiency.[14] To optimize bandwidth, lower ε_r (< 10) substrates are typically utilized in industry with polymeric substrates popular for low cost components and Al_2O_3 for high performance antennas.[15,16] However, despite their importance few commercial antennas optimize the properties of the substrate and tend to view it as a passive component whose primary purpose is to support the metallization.[15-17] Quartz and Al_2O_3 have exceptional MW properties[18-21] and are ideal as substrates for planar antenna architecture but are expensive because they are fabricated at high temperature (above 1600 ºC), polished flat if metallization losses are to be minimized (rough

surfaces induce high losses by creating an uneven metal/ceramic interface) and cannot be formed easily into complex shapes. With the development of low temperature co-fired ceramics (LTCC) technology,[8-10] dielectric and inner electrode materials are co-fired together, which decreases the fabrication time and cost, and increases the reliability of highly integrated devices. LTCC technology requires Al_2O_3 to be sintered below 961 °C (melting point of Ag) which is achieved by the addition of glass based sintering aids but which decrease *Qf*.[22-24] Recently, novel ultra-low temperature co-fired ceramics (ULTCC) technology has focused on exploring dielectric materials with intrinsic low sintering temperature and a series of novel dielectric materials that can be densified below 550 °C have been explored, such as $BaTe_4O_9$, Li_2MoO_4 and $NaAgMoO_4$.[25-29]

An ideal antenna substrate material for high performance broadband antenna applications should therefore have a low sintering temperature, a small ε_r to maximize bandwidth, a high *Qf* (>30,000), a low TCF and be chemically compatible with Ag. In this contribution, we present the sintering behavior, crystal structure, microwave dielectric properties of $Li_6B_4O_9$ ceramic in the $Li_2O-B_2O_3$ binary system fabricated by different processing routes. In addition, a prototype patch antenna using $Li_6B_4O_9$ ceramic as a substrate was designed, simulated and then fabricated by tape casting, screen printing and LTCC technology.

Experimental Section

Sample Synthesis. Proportionate amounts of reagent-grade starting materials of $LiBO_2$, H_3BO_3, B_2O_3 and Li_2CO_3 (> 99.9%, Sigma-Aldrich) were measured according to the stoichiometric formulation $Li_6B_4O_9$. Powders were mixed and ball-milled 24 h in isopropanol. The powder mixture was dried and calcined 4h at 580 °C. The

calcined powders were re-milled 24 h and pressed into cylinders (13 mm diameter and 4 ~ 5 mm high) at 50 MPa. Samples were sintered 2 h between 600 ^{o}C and 650 ^{o}C.

Structural and Microstructural Characterizations. X-ray diffraction (XRD) was performed using with CuKα radiation (Bruker D2 Phaser) from 5-65° 2θ at a step size of 0.02 ^{o}. The results were analyzed by the Rietveld profile refinement method, using a FULLPROF program. Thermally etched surfaces were observed using a scanning electron microscopy (SEM, FEI, Inspect F).

Microwave Dielectric Property and Antenna Measurement. Dielectric properties at microwave frequency were measured with the $TE_{01\delta}$ dielectric resonator method[30] using a network analyzer (Advantest R3767CH; Advantest, Tokyo, Japan) and a home-made heating system. The temperature coefficient of resonant frequency TCF (τ_f) was calculated with the following formula:

$$TCF(\tau_f) = \frac{f_{85} - f_{25}}{f_{25} \times (85 - 25)} \times 10^6 \quad (1)$$

where f_{85} and f_{25} are the $TE_{01\delta}$ resonant frequencies at 85 ^{o}C and 25 ^{o}C, respectively. Transmission parameter S_{11} was also measured using the same network analyzer. Design and simulation of the antenna were performed using CST MICROWAVE STUDIO software.

Results and Discussions

The $Li_2O-B_2O_3$ binary diagram has been studied for more than 50 years and shows great complexity (Fig. S1)[31-35] with ~ 10 compounds some of which are high temperature or pressure induced polymorphs.[36] Within industry, solid state reaction is preferred over soft chemical routes for the fabrication of ceramics due to its low cost and ease of scale up. However, the raw material source of B_2O_3 is problematic for the

fabrication of borate compounds. H_3BO_3 and B_2O_3 were initially utilized for the fabrication of borates but trials quickly illustrated that loss of B_2O_3 due to solubility in aqueous environments and through volatilization was a major issue, leading to the formation of $Li_4B_2O_5$, Fig. S2. Excess H_3BO_3/B_2O_3 was used to compensate for the loss of B_2O_3 but this resulted in the formation of lithium metaborate ($LiBO_2$) as shown in Fig. S2. However, the relative ease with which $LiBO_2$ forms and its stability in ambient suggests that this compound is an ideal reagent for the formation of $Li_6B_4O_9$ through reaction with Li_2CO_3, according to the following equation:

$$4LiBO_2 + Li_2CO_3 \xrightarrow{600^oC} Li_6B_4O_9 + CO_2 \uparrow \quad (2)$$

Fig. 1 shows XRD traces of $Li_6B_4O_9$ ceramics sintered using Li_2CO_3 and $LiBO_2$ in the appropriate proportions. All peaks were attributed to $Li_6B_4O_9$ phase when sintered at 600°C with no secondary phases. Moreover, near full density could be obtained at 630 °C, indicating that $LiBO_2$ is a superior starting material, with respect to H_3BO_3 and B_2O_3, for the formation of $Li_6B_4O_9$. Crystal structure refinements were performed on powder samples using Fullprof software and the results are shown in Fig. 1b. The refined cell parameters are a = 3.334(9) Å, b =23.487(0) Å, c = 9.202(9) Å and β = 92.650(2) ° with R_p = 5.17 %, R_{wp} = 6.98 %, and R_{exp} = 4.60 % (the goodness of fit is defined as S = R_{wp} / R_{exp} = 1.52), similar to values reported in the literature.[37] The cell volume is 720.06(4) $Å^3$ and the theoretical density is ~ 2.112 g/cm^3. There are four formula units per cell and the Li, B and O atoms are distributed on the Wyckoff general position 4e, with full occupancy. A schematic of its crystal structure is inset in Fig. 1b, in which four B atoms are located in the middle of a regular triangle, forming planar BO_3 units, linked by vertices to form quasi-planar B_4O_9 groups made of four BO_3. Lithium atoms are coordinated only by oxygen atoms belonging to B_4O_9 groups and located in distorted tetrahedra and in trigonal bipyramids. The refined atomic

fractional coordinates from XRD data are listed in Table S1.

To study compatibility with potential electrodes, mixtures of $Li_6B_4O_9$ and 15 wt.% silver / aluminum powders were co-fired at 630 °C for 2 h. For samples co-fired with silver (Fig. 1), only XRD peaks associated with $Li_6B_4O_9$ and silver were revealed, from which we conclude that $Li_6B_4O_9$ ceramics are chemically compatible with silver. However, for samples co-fired with aluminum, Li_2AlBO_4 and $Li_3AlB_2O_6$ peaks were detected in addition to $Li_6B_4O_9$ and aluminum. We therefore suggest the following possible reactions:

$$2Li_6B_4O_9 + 6Al \xrightarrow{630^oC} 6Li_2AlBO_4 + B_2O_3 \quad (3)$$

$$2Li_6B_4O_9 + 4Al + 3O_2 \xrightarrow{630^oC} 4Li_3AlB_2O_6 \quad (4)$$

The reaction of $Li_6B_4O_9$ with aluminum in air to form $Li_3AlB_2O_6$ occurs with a stoichiometric ratio of Li and B with respect to the starting composition. However, due to inhomogeneity, Li_2AlBO_4 may also react with more aluminum along with amorphous B_2O_3 to form $Li_3AlB_2O_6$. Irrespective of the precise reaction, it is evident that $Li_6B_4O_9$ reacts strongly with aluminum at 630 °C.

An SEM image of a thermally etched surface of $Li_6B_4O_9$ ceramic is shown in Fig. 2a which reveals a dense microstructure with bar-shape grains (2 ~ 5 μm in length). A BEI image of $Li_6B_4O_9$ ceramic that reacted for 2 h at 630 °C with 15 wt. % silver is shown in Fig. 2b. Two types of grains with different contrasts are observed. The weight average atomic number of silver is much larger than that of $Li_6B_4O_9$ and thus these two phases have bright and dark contrast, respectively, as shown in Fig. 2b. There is no evidence of reaction between silver and $Li_6B_4O_9$, further confirming their chemical compatibility.

Bulk density of the $Li_6B_4O_9$ ceramic sintered at 600 °C was 1.873 g/cm^3, giving a relative density of ~ 88.66 %. When the sintering temperature increased to 640 °C,

optimal density ~ 2.003 g/cm^3 (94.8 % relative density) was obtained and commensurate with an increase in ε_r (5.95) and *Qf* (41,800 GHz) but TCF (− 73 ppm/^{o}C) remained almost constant. Ceramic can be treated as composite containing grains and pores. The permittivity of pore is 1, which is usually much smaller than that of oxide ceramic. Hence, the microwave dielectric permittivity of the $Li_6B_4O_9$ ceramic followed the similar change trend to that of relative density and a maximum value ~ 5.95 was reached at 640 ^{o}C. Shannon's additive rule[38] may be utilized to establish the theoretical ε_r of the matrix phase. The molecular polarizabilities (α) in microwave region may be estimated by summing α of the constituent ions as follows:

$$\alpha(\mathrm{Li_6B_4O_9}) = 6\alpha_{Li^{3+}} + 4\alpha_{B^{3+}} + 9\times\alpha_{O^{2-}} = 25.49 \text{ Å} \quad (5)$$

where $\alpha_{Li^{3+}}$, $\alpha_{B^{3+}}$ and $\alpha_{O^{2-}}$ are the respective polarizabilities of Li^{3+} (1.2 Å^3), B^{3+} (0.05 Å^3) and O^{2+}(2.01 Å^3) ions.[38] Considering the Clausius–Mosotti relation:[39]

$$\varepsilon = \frac{3V + 8\pi\alpha}{3V - 4\pi\alpha}, \quad (6)$$

where V is the cell volume (720.06/4), the calculated permittivity is ~ 5.37, 10 % smaller than the measured value. Microwave dielectric losses include intrinsic and extrinsic parts.[40-42] with the former determined by its crystal structure and representing the upper limit of *Qf*. The latter is caused by defects and can be minimized by optimal processing.

Al_2O_3 based substrates are used commercially for the fabrication of radio frequency (RF) devices. Un-doped Al_2O_3 has a sintering temperature > 1600 ^{o}C with a ε_r ~ 10, *Qf* > 600,000 GHz and TCF − 60 ppm/^{o}C.[40,43] To meet the requirement of LTCC, glass frits are added to Al_2O_3 to lower its sintering temperature below 960 ^{o}C accompanied by serious deterioration of *Qf*. Compared with Al_2O_3-based ceramics, $Li_6B_4O_9$ has a much lower sintering temperature (~ 630 ^{o}C) and small ε_r (~ 5.95).

Table I shows a series of ultra-low sintering temperature microwave dielectric ceramics with $4.2 \leq \varepsilon_r \leq 10.2$. Among them, $Li_6B_4O_9$ exhibits competitive *Qf* and chemical compatibility with silver electrodes.[44-47] In addition, $Li_6B_4O_9$ ceramic has the lowest bulk density among all the reported microwave dielectric ceramics and therefore enables light-weighting of devices. The $Li_3AlB_2O_6$ also has a small bulk density (2.385 g/cm^3) but its relative density is only ~ 88 % in ceramics sintered at 655 ^oC. Figure S3 and S4 show the dielectric properties of commercial A6 materials[48] from Ferro in comparison with $Li_6B_4O_9$ ceramics over a wide frequency range. Although different measurement methods were employed, Fabry-Perot resonant method[49] for A6 and $TE_{01\delta}$ method for $Li_6B_4O_9$ ceramic, $Li_6B_4O_9$ ceramics possess a lower dielectric loss (< 20 GHz) in addition to a lower sintering temperature. The large cell volume (720.06(4) Å^3) and small atomic weights of both Li and B determine the small bulk density of $Li_6B_4O_9$ ceramic. The low sintering temperature of $Li_6B_4O_9$ ceramic is determined by its low melting/decomposition temperature about 700 ^oC. In the $Li_6B_4O_9$ compounds, the B atoms possess sp2 hybrid orbital which prefer to be bonded within plane structures, as the case here along [bc] planes, and this specific crystal structure makes it easy to be moved between [bc] planes at low temperatures,[37] resulting in low densification temperature of ceramic samples. However, the TCF value of $Li_6B_4O_9$ ceramic is still too large to be employed in applications. Addition of other microwave dielectric ceramics with positive TCF values might help achieve temperature stable composite ceramics, as the case in Al_2O_3-TiO_2 system.[50,51] In combination, its low density (lighter weight per device), small ε_r, high *Qf*, ultra-low sintering temperature and chemical compatibility with Ag make $Li_6B_4O_9$ a promising microwave dielectric substrate for 5G applications.

Microwave dielectric ceramics with low permittivity values are suitable for

substrate application due to its small propagation delay, which is proportional to the square root of permittivity. To demonstrate its potential, a patch antenna was designed using CST software with $Li_6B_4O_9$ as substrate as shown in Fig. 4a. Silver paste was screen-printed on the surface of a green $Li_6B_4O_9$ body and co-fired at 630 ^oC following with an SMA connect assembled. The optical image of the final prototype is inset in Fig. 4a. A representative SEM cross section of the co-fired sample is also inset in Fig. 4a, from which clear boundary between dielectric and electrode layers can be observed. The simulated and measured S_{11} parameters are shown in Fig. 4b. The simulated resonant frequency is 4.262 GHz and the simulated bandwidth is 308 MHz (based on $S_{11} < -10$ dB). The measured result shows that the antenna resonates at 4.255 GHz and has a bandwidth of ~ 279 MHz. The center frequencies of simulated and measured results are therefore, similar but the measured bandwidth is ~ 9 % smaller than that of simulated value.

Conclusions

Compared with the B_2O_3 and H_3BO_3, $LiBO_2$ is a more effective starting reagent to synthesize $Li_6B_4O_9$ via solid state reaction at 600 ^oC. Dense ceramics were obtained at 640 ^oC with a bulk density ~ 2.003 g/cm^3 (relative density ~ 94.8 %) and ε_r ~ 5.95, *Qf* ~ 41,800 GHz and TCF ~ − 72 ppm/^oC. A prototype patch antenna was fabricated by exploiting $Li_6B_4O_9$ compatibility with silver metallization using LTCC technology. Good agreement of measured and simulated values of transmission parameter S_{11} were obtained with a resonant frequency ~ 4.255 GHz and a bandwidth ~ 279 MHz.

ASSOCIATED CONTENT

Supporting Information

We added the phase diagram of Li_2O-B_2O_3, XRD patterns of $Li_6B_4O_9$ powders using H_3BO_3/B_2O_3 as initial materials, and dielectric properties of the $Li_6B_4O_9$ ceramics as a function of frequency (9.5~ 14.7 GHz) in supporting information.

The Supporting Information is available free of charge on the ACS Publications website at DOI:

AUTHOR INFORMATION

Corresponding Author

*E-mail: zhoudi1220@gmail.com

*E-mail: i.m.reaney@sheffield.ac.uk

ORCID

Di Zhou: 0000-0001-7411-4658

Dawei Wang: 0000-0001-6957-2494

Ian M. Reaney: 0000-0003-3893-6544

Notes

The authors declare no competing financial interest.

ACKNOWLEDGEMENTS

This work was supported by the United Kingdom Research Institute (UKRI) grants EP/L017563/1 and EP/N010493/1, the National Key Research and Development Program of China (2017YFB0406301), the National Natural Science Foundation of China (U1632146), the Young Star Project of Science and Technology of Shaanxi

Province (2016KJXX-34), the Key Basic Research Program of Shaanxi Province (2017GY-129), the Fundamental Research Funds for the Central University, and the 111 Project of China (B14040).

REFERENCES

(1) Ashton, K. That 'Internet of Things' Thing. *Rfid J.* **2009**, 06-22.

(2) Atzori, L.; Iera, A.; Morabito, G. The Internet of Things: A survey. *Comput. Netw.* **2010**, *54*, 2787-2805, DOI 10.1016/j.comnet.2010.05.010.

(3) Miorandi, D.; Sicari, S.; De Pellegrini, F. Internet of things: Vision, applications and research challenges. *Ad Hoc Networks* **2012**, *10*, 1497-1516, DOI 10.1016/j.adhoc.2012.02.016.

(4) Chou, K. C. Some remarks on protein attribute prediction and pseudo amino acid composition. *J. Theor. Biol.* **2011**, 273, 236-247, DOI 10.1016/j.jtbi.2010.12.024.

(5) Ganti, R. K.; Ye, F.; Lei, H. Mobile Crowdsensing: Current State and Future Challenges. *IEEE Commun. Mag.* **2011**, *49*, 32-39, DOI 10.1109/MCOM.2011.6069707.

(6) Mirsaneh, M.; Leisten, O. P.; Zalinska, B.; Reaney, I. M. Circularly Polarized Dielectric- Loaded Antennas: Current Technology and Future Challenges. *Adv. Funct. Mater.* **2008**, *18*, 2293-2300, DOI 10.1002/adfm.200701444.

(7) Li W. B.; Zhou D. Enhanced energy storage density by inducing defect dipoles in lead free relaxor ferroelectric $BaTiO_3$ based ceramics. *Appl. Phys. Lett.* **2017**, *110*, 132902, DOI 10.1063/1.4979467.

(8) Sebastian, M. T.; Jantunen, H. Low loss dielectric materials for LTCC applications: a review. *Int. Mater. Rev.* **2008**, *53*, 57-90, DOI 10.1179/174328008X277524.

(9) Sebastian, M. T.; Ubic, R.; Jantunen, H. Low-loss dielectric ceramic materials and their properties. *Int. Mater. Rev.* **2015**, *60*, 392-412, DOI 10.1179/1743280415Y.0000000007.

(10) Zhou, D.; Pang, L. X.; Wang, D. W.; Li, C.; Jin, B. B.; Reaney, I. M. High

permittivity and low loss microwave dielectrics suitable for 5G resonators and low temperature co-fired ceramic architecture. *J. Mater. Chem. C* **2017**, *5*, 10094-10098, DOI 10.1039/C7TC03623J.

(11) Zhou, D.; Guo, D.; Li, W. B.; Pang, L. X.; Yao, X.; Wang, D. W.; Reaney, I. M. Novel temperature stable high-εr microwave dielectrics in the Bi_2O_3–TiO_2–V_2O_5 system. *J. Mater. Chem. C* **2016**, *4*, 5357-5362, DOI 10.1039/C6TC01431C.

(12) Reaney, I. M.; Iddles, D. M. Microwave Dielectric Ceramics for Resonators and Filters in Mobile Phone Networks. *J. Am. Ceram. Soc.* **2006**, *89*, 2063-2072, DOI 10.1111/j.1551-2916.2006.01025.x.

(13) Zhou, D.; Wu, W.; Wang, H.; Jiang, Y.; Yao, X. The two element antennas using $BiNbO_4$ ceramics as the substrate. *Mater. Sci. Eng. A* **2007**, *460*, 652-655, DOI 10.1016/j.msea.2007.02.050.

(14) Huynh, A. P.; Long, S. A.; Jackson, D. R. Effects of Permittivity on Bandwidth and Radiation Patterns of Cylindrical Dielectric Resonator Antennas. *Ant. Prop. Soc. Int. Symp. (APSURSI) IEEE*, **2010**, 1-4, DOI 10.1109/APS.2010.5562338.

(15) Hall, P. S.; Wood, C.; Garrett, C. Wide bandwidth microstrip antennas for circuit integration. *Electronics Let.* **1979**, *15*, 458-460, DOI 10.1049/el:19790329.

(16) Ullah, M. H.; Islam, M. T. Design of a Modified W-shaped patch antenna on Al_2O_3 ceramic materials substrate for Ku-band. *Chalcogenide Lett.* **2012**, *9*, 61-66.

(17) Yang, F.; Rahmat-Samii, Y. Reflection phase characterizations of the EBG ground plane for low profile wire antenna applications. *Trans. Antennas Propagat.* **2003**, *51*, 2691-2703, DOI 10.1109/TAP.2003.817559.

(18) Ohsato, H.; Tsunooka, T.; Ando, M.; Ohishi, Y.; Miyauchi, Y.; Kakimoto, K. Millimeter-wave Dielectric Ceramics of Alumina and Forsterite with High Quality

factor and Low Dielectric Constant. *J. Korean Ceram. Soc.* **2003**, *40*, 350-353, DOI 10.4191/KCERS.2003.40.4.350.

(19) Lim, M. H.; Park, J. H.; Kim, H. G.; Yoo, M. J. *Proc. IEEE Int. Conf. on 'Properties and applications of dielectric materials'*, **2003**, *2*, 757-760.

(20) Seo, J. J.; Shin, D. J.; Cho, Y. S. Phase Evolution and Microwave Dielectric Properties of Lanthanum Borate- Based Low- Temperature Co-Fired Ceramics Materials. *J. Am. Ceram. Soc.* **2006**, *89*, 2352-2355, DOI 10.1111/j.1551-2916.2006.01035.x.

(21) Ahamdi, M. R. N.; Safavi-Naeini, S. *IEEE Antennas and Propagation Society International Symposium*, **2007**, 4598-4601.

(22) Chen, C. L.; Wei, W. J.; Roosen, A. Wetting, densification and phase transformation of $La_2O_3/A_2O_3/B_2O_3$-based glass–ceramics. *J. Eur. Ceram. Soc.* **2006**, *26*, 59-65, DOI 10.1016/j.jeurceramsoc.2004.10.001.

(23) Chakraborty, I. N.; Shelby, J. E.; Condrate, R. A. Properties and structure of lanthanum borate glasses. *J. Am. Ceram. Soc.* **1984**, *67*, 782-785, DOI 10.1111/j.1151-2916.1984.tb19700.x.

(24) Dai, S.; Huang, R. F.; Wilcox, D. L. Use of titanates to achieve a temperature-stable low-temperature cofired ceramic dielectric for wireless applications. *J. Am. Ceram. Soc.* **2002**, *85*, 828-832, DOI 10.1111/j.1151-2916.2002.tb00179.x.

(25) Sebastian, M. T.; Wang, H.; Jantunen, H. Low temperature co-fired ceramics with ultra-low sintering temperature: A review. *Curr. Opin. Solid State Mater. Sci.* **2016**, *20*, 151-170, DOI /10.1016/j.cossms.2016.02.004.

(26) Zhou, D.; Randall, C. A.; Pang, L. X.; Wang, H.; Guo, J.; Zhang, G. Q.; Wu, X. G.; Shui, L.; Yao, X. Microwave Dielectric Properties of Li_2WO_4 Ceramic with

Ultra-Low Sintering Temperature. *J. Am. Ceram. Soc.* **2011**, *94*, 348-450, DOI 10.1111/j.1551-2916.2010.04312.x.

(27) Kwon, D. K.; Lanagan, M. T.; Shrout, T. R. Microwave Dielectric Properties and Low- Temperature Cofiring of $BaTe_4O_9$ with Aluminum Metal Electrode. *J. Am. Ceram. Soc.* **2005**, *88*, 3419-3422, DOI 10.1111/j.1551-2916.2005.00613.x.

(28) Zhou, D.; Randall, C. A.; Wang, H.; Pang, L. X.; Yao, X. Microwave Dielectric Ceramics in Li_2O-Bi_2O_3-MoO_3 System with Ultra- Low Sintering Temperatures. *J. Am. Ceram. Soc.* **2010**, *94*, 1096-1100, DOI 10.1111/j.1551-2916.2009.03526.x.

(29) Zhou, D.; Pang, L. X.; Qi, Z. M.; Jin, B. B. Novel ultra-low temperature co-fired microwave dielectric ceramic at 400 degrees and its chemical compatibility with base metal. *Sci. Rep.* **2014**, *4*, 5980, DOI 10.1038/srep05980.

(30) Krupka, J. Frequency domain complex permittivity measurements at microwave frequencies. *Meas. Sci. Technol.* **2006**, *17*, R55-R70, DOI 10.1088/0957-0233/17/6/R01.

(31) Sastry, B. S. R.; Hummel, F. A. Studies in Lithium Oxide Systems: I, Li_2O B_2O_3–B_2O_3. *J. Am. Ceram. Soc.* **1958**, *41*, 7-17, DOI 10.1111/j.1151-2916.1958.tb13496.x.

(32) Sastry, B. S. R.; Hummel, F. A. Studies in Lithium Oxide Systems: V, Li_2O-B_2O_3. *J. Am. Ceram. Soc.* **1959**, *42*, 216-218, DOI 10.1111/j.1151-2916.1959.tb15456.x.

(33) Wright, A. C. Borate structures: crystalline and vitreous. *Phys. Chem. Glasses: Eur. J. Glass Sci. Technol. Part B* **2010**, *51*, 1-39.

(34) Ferlat, G.; Seitsonen, A. P.; Lazzeri, M.; Mauri, F. Hidden polymorphs drive vitrification in B_2O_3. *Nat. Mater.* **2012**, *11*, 925-929, DOI 10.1038/nmat3416.

(35) Touboul, M.; Penin, N.; Nowogrocki, G. Borates: a survey of main trends concerning crystal-chemistry, polymorphism and dehydration process of alkaline

and pseudo-alkaline borates. *Solid State Sci.* **2003**, *5*, 1327-1342, DOI 10.1016/S1293-2558(03)00173-0.

(36) Neumair, S. C.; Vanicek, S.; Kaindl, R.; Többens, D. M.; Wurst, K.; Huppertz, H. High-pressure synthesis and crystal structure of the lithium borate HP-LiB_3O_5. *J. Solid State Chem.* **2011**, *184*, 2490-2497, DOI 10.1016/j.jssc.2011.07.011.

(37) Rousse, G.; Baptiste, B.; Lelong, G. Crystal Structures of $Li_6B_4O_9$ and $Li_3B_{11}O_{18}$ and Application of the Dimensional Reduction Formalism to Lithium Borates. *Inorg. Chem.* **2014**, *53*, 6034-6041, DOI 10.1021/ic500331u.

(38) Shannon, R. D. Dielectric polarizabilities of ions in oxides and fluorides. *J. Appl. Phys.* **1993**, *73*, 348-366, DOI 10.1063/1.353856.

(39) Rysselberghe, P. V. Remarks concerning the Clausius-Mossotti Law. *J. Phys. Chem.* **1932**, *36*, 1152-1155, DOI 10.1021/j150334a007.

(40) Penn, S. J.; Alford, N. M.; Templeton, A.; Wang, X.; Xu, M.; Reece, M.; Schrapel, K. Effect of Porosity and Grain Size on the Microwave Dielectric Properties of Sintered Alumina. *J. Am. Ceram. Soc.* **1997**, *80*, 1885-1888, DOI 10.1111/j.1151-2916.1997.tb03066.x.

(41) Zhou, D.; Pang, L. X.; Guo, J.; Qi, Z. M.; Shao, T.; Wang, Q. P.; Xie, H. D.; Yao, X.; Randall, C. A. Influence of Ce Substitution for Bi in $BiVO_4$ and the Impact on the Phase Evolution and Microwave Dielectric Properties. *Inor. Chem.* **2014**, *53*, 1048-1055, DOI 10.1021/ic402525w.

(42) Zhang, Y. D.; Zhou, D. Pseudo Phase Diagram and Microwave Dielectric Properties of Li_2O–MgO–TiO_2 Ternary System. *J. Am. Ceram. Soc.* **2016**, *99*, 3645-3650, DOI 10.1111/jace.14402.

(43) Alford, N. M.; Penn. S. J. Sintered alumina with low dielectric loss. *J. Appl. Phys.* **1996**, *80*, 5895-5898, DOI 10.1063/1.363584.

(44) Ohashi, M.; Ogawa, H.; Kan, A.; Tanaka, E. Microwave dielectric properties of low-temperature sintered $Li_3AlB_2O_6$ ceramic. *J. Eur. Ceram. Soc.* **2005**, *25*, 2877-2881, DOI 10.1016/j.jeurceramsoc.2005.03.158.

(45) Li, W. B.; Xi, H. H.; Zhou, D. Microwave dielectric properties of $LiMVO_4$ (M=Mg, Zn) ceramics with low sintering temperatures. *Ceram. Int.* **2015**, *41*, 9063-9068, DOI 10.1016/j.ceramint.2015.03.279.

(46) Zhou, D.; Randall, C. A.; Pang, L. X.; Wang, H.; Wu, X. G.; Guo, J.; Zhang, G. Q.; Shui, L.; Yao, X. Microwave Dielectric Properties of $Li_2(M^{2+})_2Mo_3O_{12}$ and $Li_3(M^{3+})Mo_3O_{12}$ (M=Zn, Ca, Al, and In) Lyonsite-Related-Type Ceramics with Ultra-Low Sintering Temperatures. *J. Am. Ceram. Soc.* **2011**, *94*, 802-805, DOI 10.1111/j.1551-2916.2010.04148.x.

(47) Chen, X.; Zhang, W.; Zalinska, B.; Sterianou, I.; Bai, S.; Reaney, I. M. Low Sintering Temperature Microwave Dielectric Ceramics and Composites Based on Bi_2O_3–B_2O_3. *J. Am. Ceram. Soc.* **2012**, *95*, 3207-3213, DOI 10.1111/j.1551-2916.2012.05295.x.

(48) Ferro, http://www.ferro.com/, (accessed on 2018/6/5).

(49) Breeden, K. H.; Langley, J. B. Fabry-Perot Cavity for Dielectric Measurements. *Rev. Sci. Instrum.* **1969**, *40*, 1162, DOI 10.1063/1.1684188.

(50) Huang, C. L.; Wang, J. J.; Huang, C. Y. Microwave Dielectric Properties of Sintered Alumina using Nano-scaled Powders of Alpha Alumina and TiO_2. *J. Am. Ceram. Soc.* **2007**, *90*, 1487-1493, DOI 10.1111/j.1551-2916.2007.01557.x.

(51) Campos, R. V. B.; Bezerra, C. L.; Oliveira, L. N. L.; Gouveia, D. X.; Silva, M. A. S.; Sombra, A. S. B. A Study of the Dielectric Properties of Al_2O_3-TiO_2 Composite in the Microwave and RF Regions. *J. Electron. Mater.* 2015, *44*, 4220-4226, DOI 10.1007/s11664-015-3958-3.

Table Captions

Table I. Sintering temperatures and microwave dielectric properties of some low permittivity LTCC materials in order of bulk density in order of density.

Composition	Density (g/cm^3)	S.T.	ε_r	*Qf* (GHz)	TCF Value (ppm/°C)	Electrode	Ref.
$Li_6B_4O_9$	**2.003**	**640**	**6.0**	**41,800**	**−72**	**♀Ag; ♂Al**	This work
$Li_3AlB_2O_6$*	2.385	650	4.2	12,460	−290	not studied	44
Li_2MoO_4	3.031	540	5.5	46,000	−160	♀Ag & Al	28
$LiMgVO_4$	3.211	675	9.1	33,730	−160	♂Ag	45
$Li_3AlMo_3O_{12}$	3.891	570	9.5	50,000	−73	♀Ag & Al	46
Li_2WO_4	4.567	640	5.5	62,000	−146	♀Ag & Al	26
$NaAgMoO_4$	4.928	400	7.9	33,000	−120	♀Ag & Al	29
$Bi_6B_{10}O_{24}$	6.183	700	10.2	10,750	−41	not studied	47

S.T.= Sintering Temperature; ♀=chemically compatible; ♂=not chemically compatible; * Relative density =88 %

Figure Captions

Fig. 1 a) XRD patterns of the $Li_6B_4O_9$ ceramic sintered at 600 ^oC, co-fired ceramics with 15 wt. % aluminum and silver, respectively, at 630 ^oC for 2 h, and b) crystal structure and Rietveld refinement of $Li_6B_4O_9$.

Fig. 2 a) SEM image of thermally etched surface of $Li_6B_4O_9$ ceramic sintered at 630 ^oC and b) BEI image of the co-fired ceramic with 15 wt. % at 630 ^oC.

Fig. 3 a) Relative density and b) microwave dielectric properties of the $Li_6B_4O_9$ ceramics as a function sintering temperature (resonant frequencies 10.4 ~ 10.9 GHz).

Fig. 4 a) Schematic, optical and SEM images of the antenna using $Li_6B_4O_9$ and silver as substrate and patterns, respectively, and b) the measured and simulated values of transmission parameter S_{11}.

TOC/Abstract Graphic

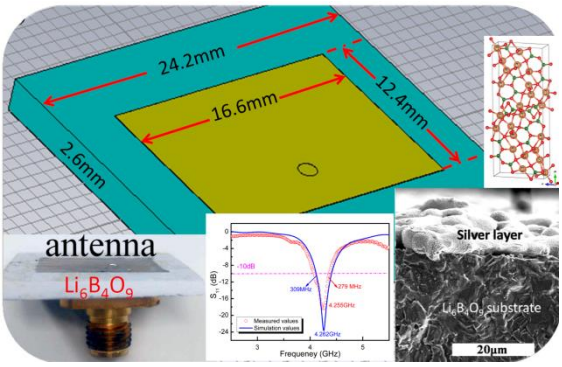

Synopsis:

$Li_6B_4O_9$ microwave dielectric ceramic can be well densified at 640 ^{o}C and a prototype patch antenna showed good transmission properties.

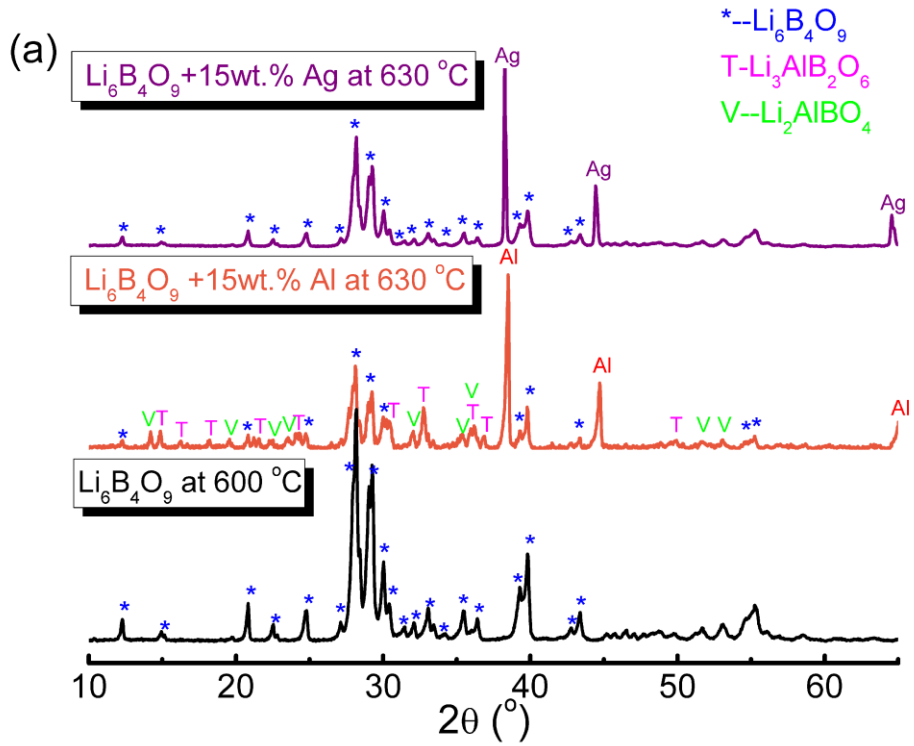
(a)
*--Li6B4O9
T-Li3AlB2O6
V--Li2AlBO4
Li6B4O9+15wt.% Ag at 630 °C
Li6B4O9 +15wt.% Al at 630 °C
Li6B4O9 at 600 °C
Ag
Al
10
20
30
40
50
60
2θ (°)

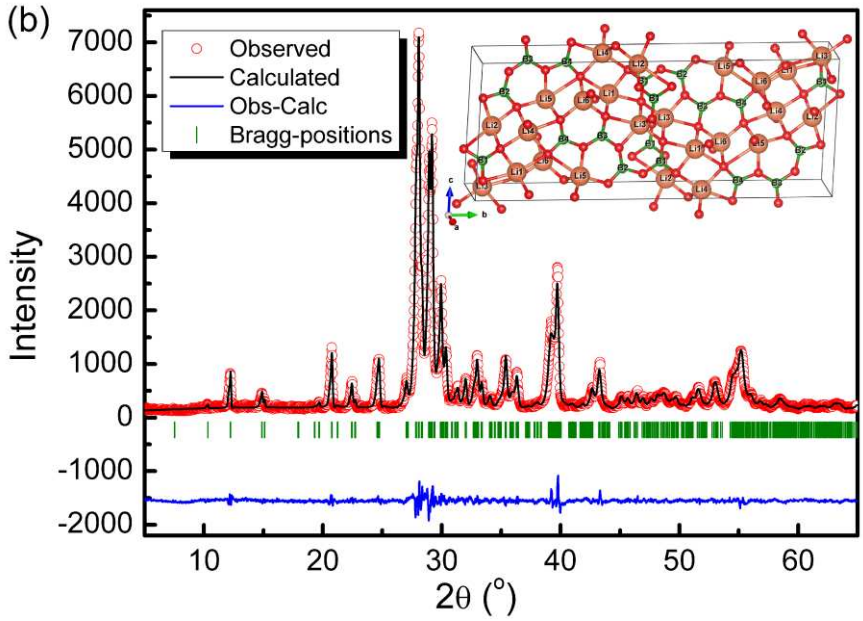
(b)
Observed
Calculated
Obs-Calc
Bragg-positions
Intensity
7000
6000
5000
4000
3000
2000
1000
0
-1000
-2000
10
20
30
40
50
60
2θ (°)

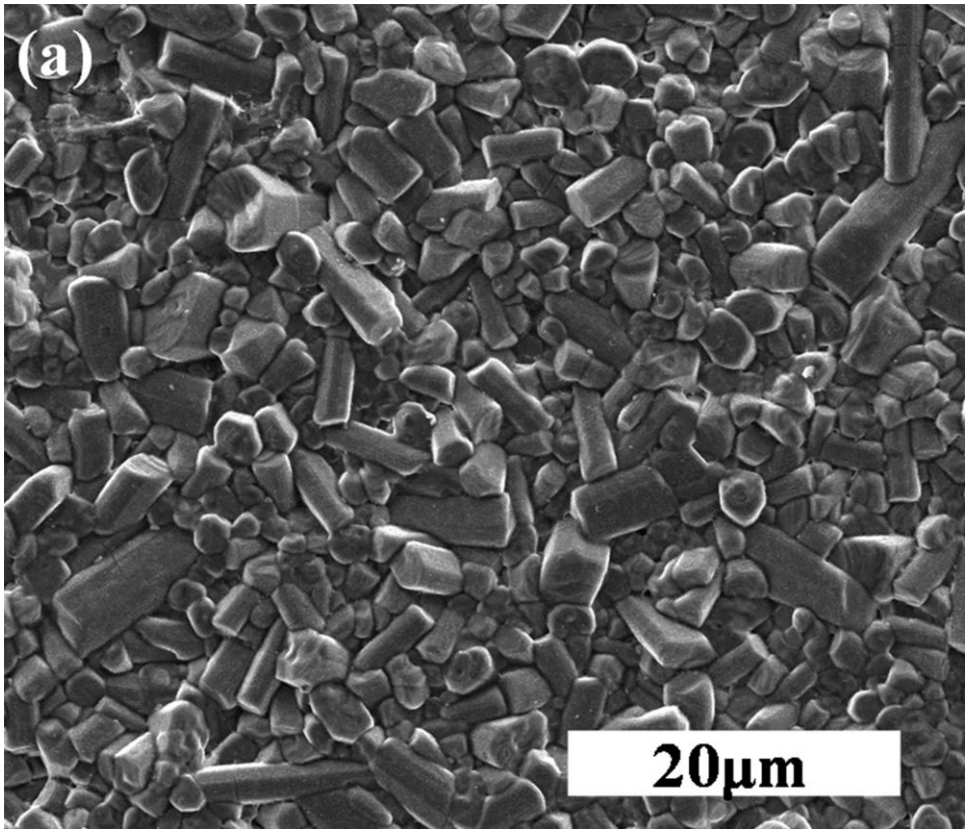
(a)
20μm

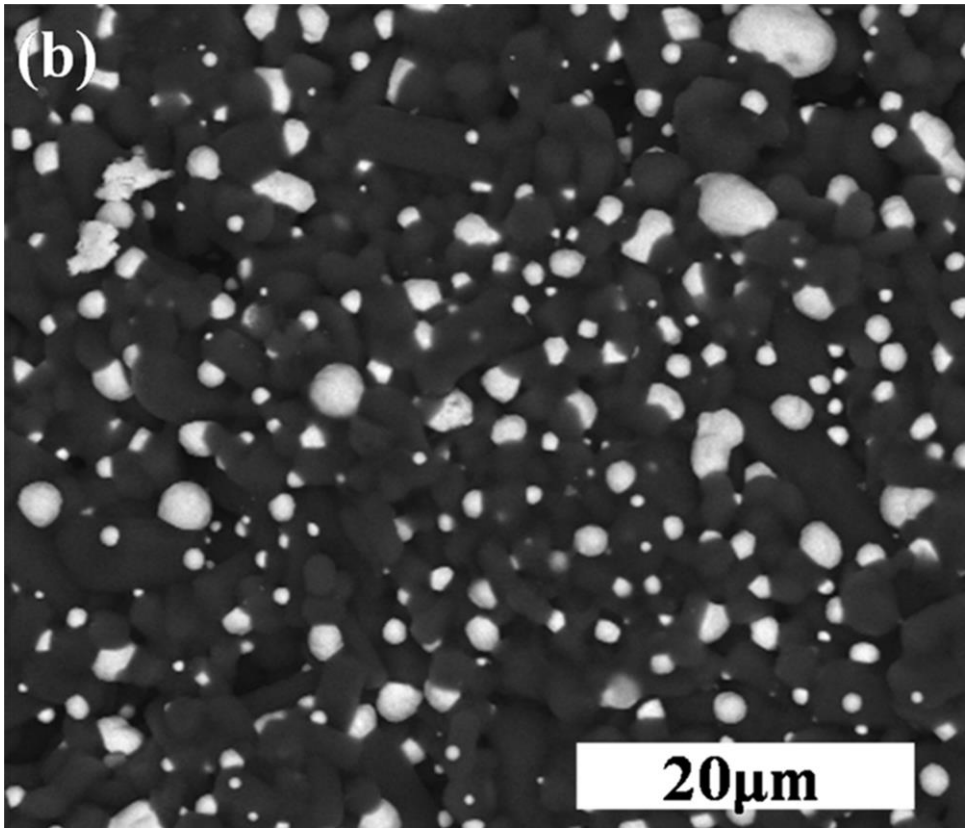
(b)
20μm

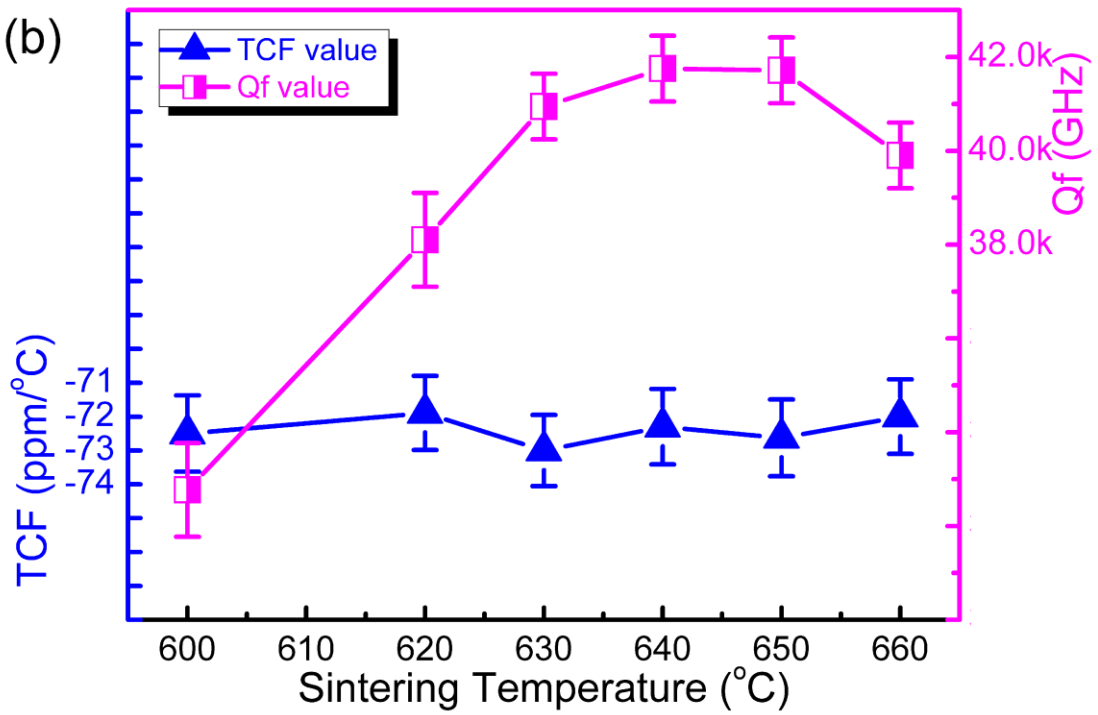
(b)
TCF value
Qf value
TCF (ppm/°C)
-71
-72
-73
-74
Qf (GHz)
42.0k
40.0k
38.0k
600
610
620
630
640
650
660
Sintering Temperature (°C)

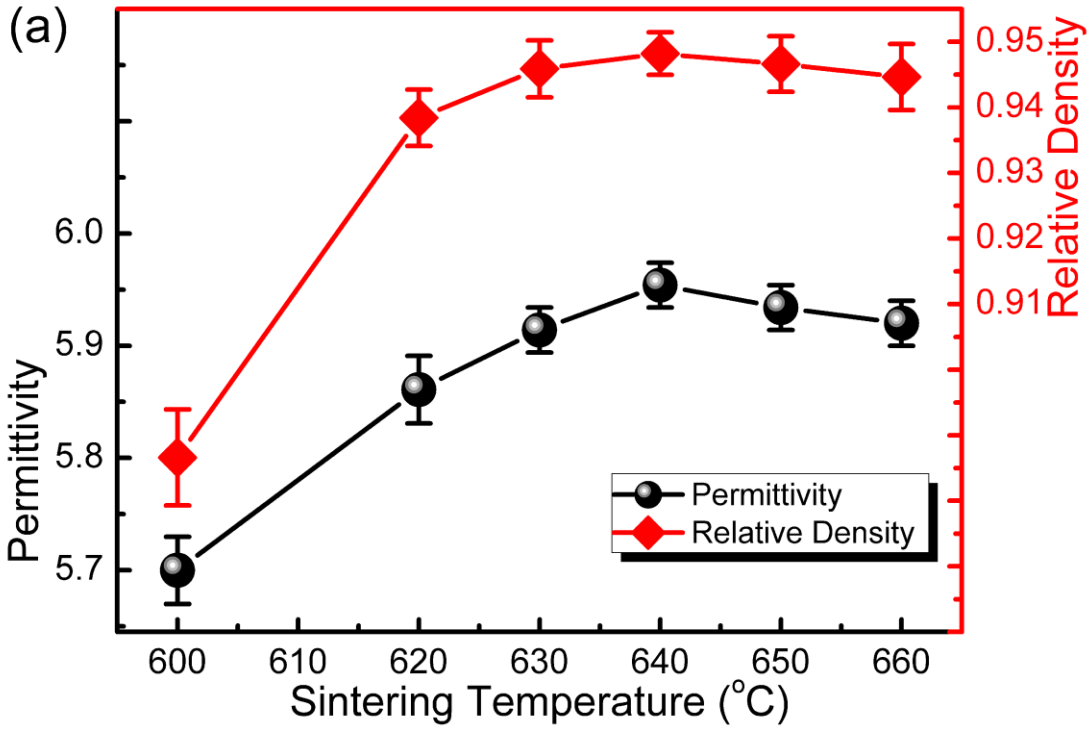
(a)
Permittivity
6.0
5.9
5.8
5.7
Relative Density
0.95
0.94
0.93
0.92
0.91
Permittivity
Relative Density
600
610
620
630
640
650
660
Sintering Temperature (°C)

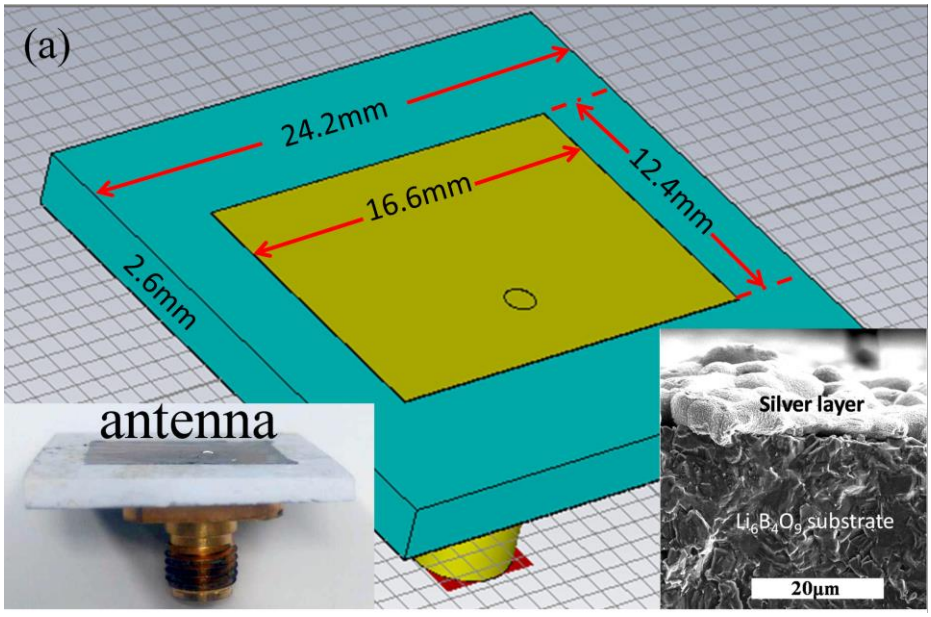
(a)
24.2mm
16.6mm
12.4mm
2.6mm
antenna
Silver layer
$Li_6B_4O_9$ substrate
20μm

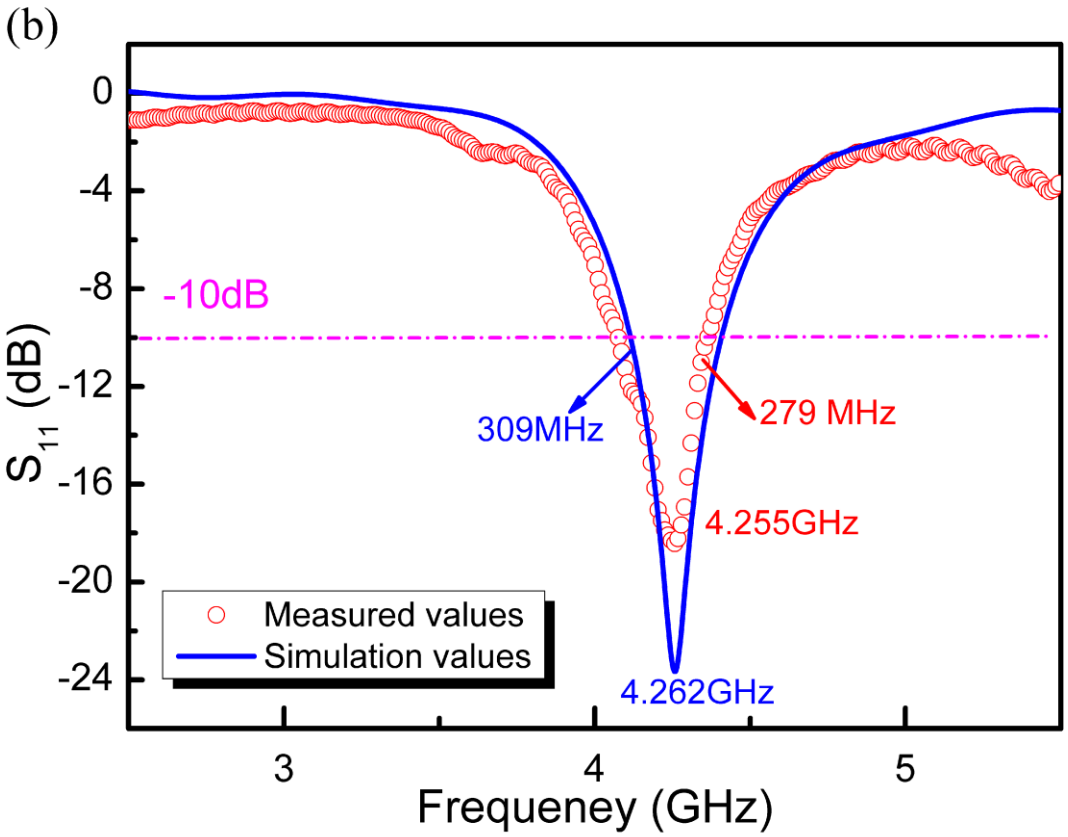
(b)
0
-4
-8
-12
-16
-20
-24
S_{11} (dB)
-10dB
309MHz
279 MHz
4.255GHz
4.262GHz
Measured values
Simulation values
3
4
5
Frequeney (GHz)